Environmental Modelling and Software 140 (2021) 105015

Contents lists available at ScienceDirect

Environmental Modelling and Software

journal homepage: http://www.elsevier.com/locate/envsoft

Quantarctica, an integrated mapping environment for Antarctica, the Southern Ocean, and sub-Antarctic islands

Kenichi Matsuoka [a,*], Anders Skoglund [a], George Roth [a], Jean de Pomereu [b], Huw Griffiths [c], Robert Headland [b], Brad Herried [d], Katsuro Katsumata [e], Anne Le Brocq [f], Kathy Licht [g], Fraser Morgan [h,i], Peter D. Neff [j], Catherine Ritz [k], Mirko Scheinert [l], Takeshi Tamura [m], Anton Van de Putte [n], Michiel van den Broeke [o], Angela von Deschwanden [a,2], César Deschamps-Berger [a,1], Brice Van Liefferinge [a], Stein Tronstad [a], Yngve Melvær [a]

[a] Norwegian Polar Institute, Tromsø, Norway
[b] Scott Polar Research Institute, University of Cambridge, Cambridge, UK
[c] British Antarctic Survey, Cambridge, UK
[d] Polar Geospatial Center, University of Minnesota, Saint Paul, MN, USA
[e] Japan Agency for Marine-Earth Science and Technology, Yokosuka, Kanagawa, Japan
[f] Geography, College of Life and Environmental Sciences, University of Exeter, Exeter, UK
[g] Indiana University Purdue University Indianapolis, Indianapolis, IN, USA
[h] Manaaki Whenua Landcare Research, Auckland, New Zealand
[i] Te Pūnaha Matatini, University of Auckland, Auckland, New Zealand
[j] Department of Soil, Water, and Climate, University of Minnesota, Saint Paul, MN, USA
[k] Univ. Grenoble Alpes, CNRS, IRD, Grenoble INP, IGE, 38000 Grenoble, France
[l] Technische Universität Dresden, Institut für Planetare Geodäsie, 01062 Dresden, Germany
[m] National Institute of Polar Research, Tachikawa, Tokyo, 190-8518, Japan
[n] Royal Belgian Institute for Natural Science, B-1000, Brussels, Belgium
[o] Institute for Marine and Atmospheric Research, Utrecht University, the Netherlands

ARTICLE INFO

Keywords:
Geographical information system
Regional analytical tool
Polar regions

ABSTRACT

Quantarctica (https://www.npolar.no/quantarctica) is a geospatial data package, analysis environment, and visualization platform for the Antarctic Continent, Southern Ocean (>40°S), and sub-Antarctic islands. Quantarctica works with the free, cross-platform Geographical Information System (GIS) software QGIS and can run without an Internet connection, making it a viable tool for fieldwork in remote areas. The data package includes basemaps, satellite imagery, terrain models, and scientific data in nine disciplines, including physical and biological sciences, environmental management, and social science. To provide a clear and responsive user experience, cartography and rendering settings are carefully prepared using colour sets that work well for typical data combinations and with consideration of users with common colour vision deficiencies. Metadata included in each dataset provides brief abstracts for non-specialists and references to the original data sources. Thus, Quantarctica provides an integrated environment to view and analyse multiple Antarctic datasets together conveniently and with a low entry barrier.

Product availability

The product is released under the CC-BY4.0 license with DOI: https://doi.org/10.21334/npolar.2018.8516e961. Quantarctica is downloadable from the Norwegian Polar Institute (ftp://ftp.quantarctica.npolar.no/), as well as from global mirrors generously provided by the Tasmanian Partnership for Advanced Computing at the University of Tasmania (ftp://quantarctica.tpac.org.au/), the Arctic and

* Corresponding author.
E-mail address: kenichi.matsuoka@npolar.no (K. Matsuoka).
[1] Current address: CESBIO, Université de Toulouse, CNES/CNRS/INRAE/IRD/UPS, Toulouse, France.
[2] deceased.

https://doi.org/10.1016/j.envsoft.2021.105015
Accepted 18 February 2021
Available online 2 March 2021

Antarctic Data Archive System at Japan's National Institute of Polar Research (https://ads.nipr.ac.jp/gis/quantarctica/), India's National Center for Polar and Ocean Research (ftp://ftp.ncaor.gov.in/), and the Polar Geospatial Center at the University of Minnesota (ftp://ftp.data.pgc.umn.edu/gis/packages/quantarctica/). All download sites and Quantarctica-friendly datasets (see Section 4.2) are listed at Quantarctica's project web page at the Norwegian Polar Institute: https://www.npolar.no/quantarctica.

1. Introduction

The Antarctic Ice Sheet and Southern Ocean are major thermal reservoirs in the earth system that significantly influence climate change (Kennicutt et al., 2015, 2019). As the amount and availability of scientific data in this region grows, and the needs of more interdisciplinary research are realized (Kennicutt et al., 2014), researchers and students increasingly require an easy-to-use, unified platform to import, display, and analyse geospatial datasets for work involving this region. Educators and logistics operators also need a convenient platform with low entry barrier to get a complete picture of these remote areas as well as develop practical tools for their work. Many such users develop their own dedicated analysis environments for individual purposes, bringing together basic data such as terrain models, satellite imagery, and scientific data from different disciplines. Unfortunately, this entails significant start-up cost and duplicated effort.

Basic Antarctic datasets, such as the Antarctic Digital Database (ADD, https://www.add.scar.org/), and the Southern Ocean Observation System Map (SOOSmap, http://www.soosmap.aq/) exist as online portals. One can download satellite data for Antarctica from the earliest such data (decades ago) through to the present (e.g., NASA's World View, https://worldview.earthdata.nasa.gov/, Polar View, https://www.polarview.aq/antarctic, and the US Geological Survey's EarthExplorer, https://earthexplorer.usgs.gov/). In addition, the Antarctic Environmental Portal (https://www.environments.aq/) provides an important link between Antarctic science and Antarctic policy, particularly in environmental management. However, being online portals, all these data sources are not immediately helpful during remote field work or a scientific cruise. One exception is Antarctic Mapping Tools (Greene et al., 2017), which provides Antarctic data that can be operated offline. However, it is limited mostly to physical science data and its analysis functions require proprietary Matlab computing software. Thus, instead of having to gather Antarctic scientific data from numerous online data portals in many file formats and geographic projections, a user-friendly system would provide pre-compiled basic Antarctic datasets in multiple disciplines and load consistently both in the office and in the field. For this purpose, the base software platform should be low cost and multiple-platform operational with little or no license restrictions to maximize benefits for the rapidly growing Antarctic research community.

In 2011, we began developing a GIS data package that can operate with modest computer capabilities so that the system is useful at remote field camps and for a wide range of users. We selected Quantum GIS (renamed to QGIS in 2013, https://qgis.org/) for the software platform, and named the data package "Quantarctica" (hereafter QA). Version 1 of QA was released in 2012. For version 2 released in 2014, we improved the glaciology and geophysics data coverage and data visualization. The Scientific Committee on Antarctic Research (SCAR), a thematic organization of the International Science Council, selected QA version 2 as a SCAR map product in 2014 (https://scar.org/resources/maps/). To respond to the Antarctic scientific community's increased interest in QA,

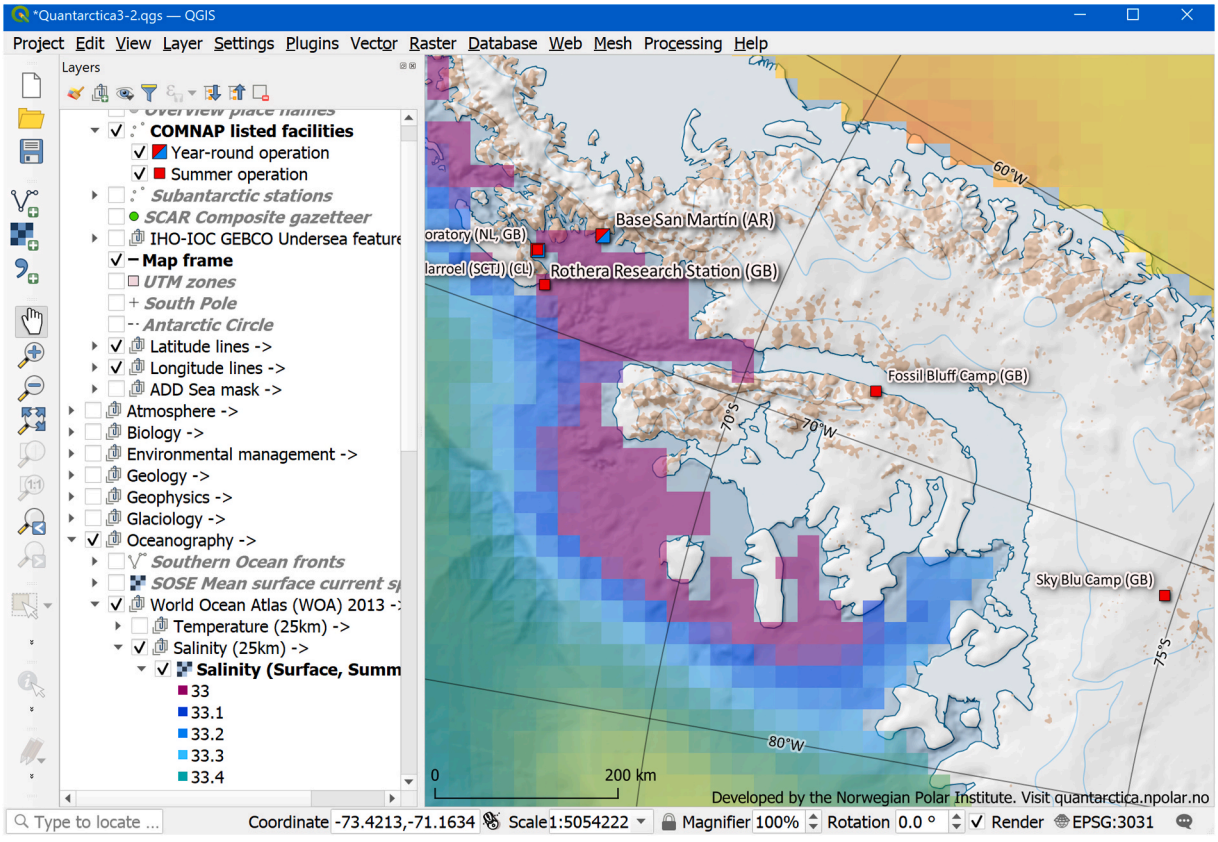

Fig. 1. Sample screenshot of Quantarctica. A QGIS interface displays both raster and vector data layers. Expandable tree options (left panel) show colour bars and legends for each data layer. The main panel at right shows the detailed basemap together with year-round and summer-only research stations, and ocean surface salinity in the summer at the scale of 1:5,054,222 (see the bottom status bar). Labels of station name and operating nation disappear when the scale goes below 1:10,000,000.

we decided to develop version 3 (QA3) with scientific data from other disciplines and expand its geographical coverage from 50°S to 40°S to include research in the Southern Ocean and Sub-Antarctic islands. QA3 was released in February 2018 for use with QGIS version 2. As our integration tests were completed, we updated QA3 to version 3.2 in 2021, which runs on QGIS version 3.16 (Fig. 1).

Here, we describe methods used to develop QA3, present the current contents of QA3, demonstrate user applications, and finally present its outlook.

2. Methods

2.1. Choice of software

To choose the base GIS software for which our data package is optimized, the following criteria were used. The software should (1) be free of charge or at least low cost, (2) work on the most common computer operating systems, (3) be able to function without an internet connection (offline readiness), (4) be relatively easy to use, (5) have a rich toolset, (6) be able to read and write common geographical-data file formats, (7) allow advanced cartography, (8) allow good map figure production, (9) be actively maintained and in development, (10) have a process that allows transparent bug-fixing processes, (11) have an active user community and rich knowledge resources, and (12) be available for bundling with the QA package (e.g., in a USB stick), for standalone offline use. We found Quantum GIS (renamed to QGIS in 2013, https://qgis.org/) to satisfy these requirements best.

2.2. Selection of data

To select data used for basemaps, miscellaneous base layers, satellite data, and terrain models, we considered Antarctic map products widely available as best suited for the purpose in the combined terms of coverage, completeness, and detail (Sections 3.1–3.4).

To select the scientific data, we first surveyed the relevant scientific community in 2016 to identify community priorities for included datasets. This input was considered by one or two editors for each discipline, and then the recommended datasets were further screened by the core development team at the Norwegian Polar Institute. QA3 includes 265 data layers, of which 164 layers represent scientific datasets (Tables 1 and 2). These selections will be re-visited when QA version 4 is developed in the future.

2.3. Mapping projection

The Antarctic Polar Stereographic projection EPSG:3031 was chosen because it is both Antarctic centric and the most commonly used projection for Antarctic geographical data already. Some datasets are originally in other projections. QGIS can handle multiple data layers projected to different systems, nonetheless, on-the-fly reprojection hampers fast rendering and demands CPU work. Therefore, all data in QA are projected to the single projection, EPSG:3031.

Table 1
Overview of the dataset.

Category	Number of data layers	Total data size (MB)
Simple/detailed basemaps	1 (simple), 24 (detailed)	1270
Miscellaneous base layers	35	339
Satellite imagery	7	2010
Terrain models	34	2120
Scientific data in 9 disciplines	164	1793
TOTAL	265	7532

Table 2
Nine scientific data disciplines.

Discipline	Number of data layers	Total data size (MB)
Atmosphere	6	5
Biology	8	76
Environmental management	9	27
Geology	9	590
Geophysics	9	20
Glaciology and ice cores	43	1050
Oceanography	50	13
Sea ice	26	11
Social science	4	1
TOTAL	164	1793

2.4. File formats, compression, and data re-sampling

Individual datasets are originally in various file formats. For consistency, we convert all vector data to ESRI shapefile format, and raster data to GeoTIFF format. Most raster files are compressed with lossless LZW and Deflate algorithms. These file formats are commonly used in the GIS community and are supported in most other GIS systems. However, including high-resolution imagery in a lossless format largely decreases QA's portability, so we converted them to the JPEG format with associated georeferenced files or to the JPEG2000 format, with a compression level that provides a hardly noticeable quality reduction (Section 3.3). These formats are less common in the GIS community but still supported widely. In this way, datasets in QA can be used in other platforms as well.

Except for re-projection, the original data are not altered.

2.5. Cartography

The presentation of data layers is carefully adjusted to be intuitive, readable and visually pleasant at all map scales. The scientific datasets are presented such as to stand out when rendered on the top of basemaps and satellite imagery. The presentation is also made so that datasets often viewed together are easily distinguishable from one another for colour-deficient users. If the predefined cartography is not fully suited for a specific purpose, QA is fully customizable, so users can change the appearance. Many data layers, particularly the detailed basemaps, use scale-dependent features so that these layers are rendered to an appropriate level of details at a given scale (Fig. 1). Most data layers constituting detailed basemaps are stored at high, medium, and low resolutions for high-performance rendering and for best cartographic expression.

2.6. Meta data

Metadata includes a brief description of the dataset for general use. Also included are original data location, citation, and the editor responsible for the data layer. We urge all users to cite this original data source, not QA, when they use the dataset in their work. In QA version 3.2, all metadata are stored as a part of the QGIS project file (.QGS file format), and in each data folder associated with individual data layers in the QMD file format. The abstract section of the metadata (brief description of the data, citation, and handling editor) is stored as plain text (TXT) files for quick reference. The latter is useful when users are interested in using specific data layers on different platforms such as ArcGIS and non-GIS platforms such as computing software R (https://www.R-project.org).

3. Results

QA3 includes datasets categorized as (1) simple and detailed basemaps, (2) miscellaneous base layers, (3) satellite imagery, (4) terrain models, and (5) a range of scientific data (Table 1). Users can display and

rearrange the order of data layers that lay on top of basemaps, satellite imagery, and terrain models at a user-chosen continuously adjustable map scale (Fig. 1). Scientific data are categorized into nine disciplines (Table 2). All data layers are stored with a folder-tree structure so that individual data files and associated metadata can be easily found. Table 3 lists all data included in QA3.

The total size of QA3's data files is 7.53 GB, with the satellite imagery and terrain models constituting about 4.13 GB (Table 1). Our distribution package with QGIS version 3.16.1 is 8.65 GB. We provide a start-up manual to adjust QGIS to the Quantarctica workspace (ftp://ftp.quantarctica.npolar.no/Quantarctica3/Quantarctica_GetStarted.pdf), which typically takes 0.5–1 h for first-time users to follow after QGIS and Quantarctica are installed.

3.1. Simple and detailed basemaps

Simple basemaps allow users to quickly render oceans, ice sheet, ice shelves, and other continents, primarily composed of the ADD data layers (Fig. 2b inset). Detailed basemaps are a composite of vector layers of ice and rock surface elevation contours, outcrops, moraines, lakes and streams, ice shelves' calving front, as well as raster layers of both bathymetry and topographic hillshade. These basemaps use the ADD and several terrain models (Figs. 1, 2b and 2c and 2d). As users zoom in, features appear with a higher resolution to balance the level of detail necessary for a given scale and rendering speed.

3.2. Miscellaneous base layers

Additional base layers show other scale-dependent features such as the 37,628 place names south of 60°S registered in the SCAR Composite Gazetteer of Antarctica (https://data.aad.gov.au/aadc/gaz/scar/). Further north, the names come from other reliable resources and shown in the language of the sovereignty. Some features are left unlabelled when the sovereignty might be disputed. Other layers show latitude/longitude lines, the Antarctic Circle, South Pole, Universal Transverse Mercator (UTM) zones, and locations and facility details of 108 research stations from a list of Antarctic facilities maintained by the Council of Managers of National Antarctic Programs (COMNAP, Fig. 1). Users can filter and search for place names and features using attribute tables. An overview place name layer gives a quick reference to large regions in a small map scale.

3.3. Satellite imagery

QA3 includes three sets of satellite imagery. One, for the Landsat images, users can view the 240-m resolution Landsat Image Mosaic of Antarctica (LIMA, taken in 1999–2002) that covers the entire ice sheet and ice shelves (Bindschadler et al., 2008), or view the 15-m resolution Landsat image tiles (taken in 2013–2017) over islands, outcrops, ice shelves, and the ice sheet except for regions ~82.7°S poleward. Two, the RADARSAT Antarctic Mapping Project's (RAMP) 100-m resolution mosaic covers the entire ice sheet and ice shelves (taken in 1997) (Jezek et al., 2013). Three is the Moderate Resolution Image Spectroradiometer (MODIS) Mosaic of Antarctica (MOA) 125-m resolution image mosaic (taken in 2003–2004) that covers the entire ice sheet and ice shelves (Haran et al., 2014; Scambos et al., 2007). These specific satellite products allow users to optimize the display of overall topographic features (LIMA, RAMP, MOA), areas of blue ice and outcrops (LIMA), and sub-surface features such as crevasses under snow detected using ice-penetrating microwaves (RAMP).

To balance image resolutions, and portability of QA, we converted LIMA to the JPEG format with associated georeferenced files and RAMP and individual Landsat tiles to the JPEG2000 format, with a compression level that provides a hardly noticeable quality reduction. To increase the rendering performance and user friendliness, more than 654 individual Landsat image tiles are combined to a single virtual mosaic file with image pyramids so that lower resolution versions are rendered when zoomed out.

3.4. Terrain models

Six terrain models are included, with spatial resolutions ranging from 0.2 to 2.0 km. Specifically, the RAMP2 (Liu et al., 2015) and CryoSat-2 (Helm et al., 2014) terrain models, as well as the ADD elevation contours, represent the surface of the outcrops, ice sheet and ice shelves (Figs. 2a and 3b). The BEDMAP2 compilation represents the ice thickness and bed topography under the ice sheet (Fretwell et al., 2013). BEDMAP2 shows uncertainties in ice thickness and bed elevation, and geographic coverage (and corresponding data sparse regions) of the ice-penetrating radar data with which ice thickness and bed elevation were determined over the ice sheet. The International Bathymetry Chart of the Southern Ocean (IBCSO) shows the bathymetry of the Southern Ocean at latitudes south of 60°S, as well as metadata on the availability and type of data used for the compilation (e.g., multibeam or single beam; Fig. 2c; Arndt et al., 2013). Finally, a global ETOPO1 relief model applies to latitudes north of 60°S (NOAA National Geophysical Data Center, 2009). Elevation references differ between the terrain models: CryoSat-2 and RAMP2 refer to the WGS84 ellipsoid, whereas the others refer to the mean sea level using different geoid models. Similarly, each terrain model has different features with different strengths and weaknesses, so users can choose the dataset that best matches their needs. All models are displayed as rasters, derived hillshades and elevation contours. Contour intervals and hillshade parameters can be customized in QGIS to better view highly variable terrains such as continental shelf breaks, abyssal plains, steep mountainous regions near the coast, and virtually flat and featureless inland ice sheet over a range of spatial scales.

3.5. Atmosphere data

Most atmospheric data provided in QA are outputs from RACMO2, a regional atmospheric climate model (van Wessem et al., 2014a, 2014b). These include near surface data, such as 2-m-high temperature and 10-m-high wind speeds over the ice sheet and ocean (Fig. 2a), as well as surface mass balance over the ice sheet and ice shelves, all annual values averaged between 1971 and 2011. The 27 km resolution RACMO2 raster datasets are originally projected in a rotated polar coordinate system which cannot easily be converted to EPSG:3031. However, each model cell has EPSG:4326 coordinate values as well, which we used to build up EPSG:3031 rasters at 35 km resolution, the best achievable without creating void data cells anywhere in between. Atmospheric data also include a dataset of satellite-observed wind scour zones over the ice sheet (Fig. 2a; Das et al., 2013). These near-surface and surface data have been selected over middle and upper atmosphere data because of their stronger influences on processes in the other disciplines.

3.6. Biology data

Biology datasets for the Southern Ocean include summer chlorophyll-a density near the ocean surface (Fig. 2b; Johnson et al., 2013; Johnson et al., 2017), 20 pelagic regions based on seawater temperature and sea-ice distribution (Raymond, 2014), and 29 benthic regions (Douglass et al., 2014). On top of these raster or polygon data layers, users can plot locations of available vertical profiles of temperature and salinity collected by the Marine Mammals Exploring the Ocean Pole to Pole project (MEOP, Fig. 2b; Treasure et al., 2017), as well as population densities of Antarctic krill and salps surveyed in 1926–2016 by 10 countries (KRILLBASE; Atkinson et al., 2017). For the Antarctic coast, data include 204 areas classified as important bird areas (IBA; Harris et al., 2016) and populations of 46 major emperor penguin colonies identified using satellite imagery (Fig. 2b; Fretwell et al., 2012).

Table 3
All data layers in Quantarctica as appeared as the tree structure.

Group	Layer or subgroup	Sub layer or layer description	Data type (Vector or Raster) and spatial resolution if raster	Reference
Miscellaneous	Overview place names		V	
	COMNAP listed facilities		V	
	Subantarctic stations		V	
	SCAR Composite gazetteer		V	
	IHO-IOC GEBCO Undersea feature names	6 differents features	V	
	Map frame		V	
	UTM zones		V	
	South Pole		V	
	Antarctic Circle		V	
	Latitude lines	Sub layers of 15', 30' 1°, 2°, 5°, 10°, 15°, 20° and 30°	V	
	Longitude lines	Sub layers of 30', 1°, 2°, 3°, 5°, 10°, 15°, 20°, 30°, 45°, and 90°	V	
	ADD Sea mask	Low, medium and high resolutions	V	
Atmosphere	Wind scour zones		V	Das et al., 2013
	RACMO Model output ->			
		RACMO Average 2m temperature	R, 35 km	van Wessem et al., 2014a
		RACMO Total sublimation	R, 35 km	van Wessem et al., 2014b
		RACMO Surface mass balance	R, 35 km	van Wessem et al., 2014b
		RACMO Total precipitation	R, 35 km	van Wessem et al., 2014b
		RACMO Average absolute 10m wind speed	R, 35 km	van Wessem et al., 2014a
Biology	MEOP Seal tracks		V	Treasure et al., 2017
	Emperor penguin colonies (2009)		V	Fretwell et al., 2012
	KRILLBASE		V	Aktinson et al., 2017
	Important Bird Areas (IBAs, BirdLife International)		V	Harris et al., 2016
	chl-a concentration ->			
		chl-a summer climatology (Johnson)	R, 9km	Johnson et al., 2017
		chl-a summer climatology (NASA)	R, 9km	Johnson et al., 2013
	Pelagic regionalisation		V	Raymond, 2014
	Benthic regionalisation		V	Douglass et al., 2014
Environmental management	Antarctic Specially Protected Areas (ASPAs, points)		V	Terauds, 2016
	Antarctic Specially Protected Areas (ASPAs, polygons)		V	Terauds, 2016
	Antarctic Specially Managed Areas (ASMAs)		V	
	Antarctic Conservation Biogeographic Regions (ACBRs)		V	Terauds et al., 2012; Terauds and Lee (2016)
	CCAMLR ->		V	
		Research Blocks	V	
		Marine Protected Areas (MPAs)	V	
		Small Scale Management Units (SSMUs)	V	
		Small Scale Research Units (SSRUs)	V	
		Statistical Areas, subareas, and divisions	V	
Geology	ADD Rock outcrop (high, Landsat8)		V	Burton-Johnson et al., 2016
	OSU BPCRC Polar Rock Repository		V	
	IBCSO Multibeam footprint		V	Arndt et al., 2013
	GeoMAP source bibliography		V	Cox et al., 2019
	USGS Earthquakes (M>2.5, 1900-2017)		V	
	Tectonic plate boundaries		V	Bird, 2003
	Tectonic plates		V	Bird, 2003
	Schematic Geological Map of Antarctica		V	Tingey, 1991
	Geomorphic features		V	Post et al., 2014
Geophysics	AntGG Gravity Anomaly Grid ->			Scheinert et al., 2016
		AntGG Accuracy	R, 10 km	
		AntGG Free-air gravity anomaly	R, 10 km	
		AntGG Bouguer anomaly	R, 10 km	
	EIGEN-6C4 Gravity Model ->			Förste et al., 2014

(*continued on next page*)

Table 3 (*continued*)

Group	Layer or subgroup	Sub layer or layer description	Data type (Vector or Raster) and spatial resolution if raster	Reference
		EIGEN-6C4 Gravity disturbance	R, 10 km	
		EIGEN-6C4 Height anomaly	R, 10 km	
	World Magnetic Model ->			Golynsky et al., 2001; Golynsky et al., 2013
		Magnetic South Pole locations (1590-2015)	V	
		Magnetic declination contours	V	
	ADMAP Magnetic anomaly		R, 5 km	Chulliat et al., 2014
	Geothermal heat flux, An		R, 5 km	An et al., 2015
Glaciology	SAMBA Surface mass balance measurements		V	Favier et al., 2013
	Ice cores database		V	
	Surface snow isotopes		V	Touzeau et al., 2016
	ASAID Grounding/ hydrostatic lines ->			Bindschadler et al., 2011
		Sub layers for grounding lines (continent)	V	
		Sub layers for grounding lines (islands)	V	
		Sub layers for hydrostatic lines (continent)	V	
		Sub layers for hydrostatic lines (islands)	V	
		ASAID Grounding line, simplified	V	
	RAISED Paleo ice extents	At 5ka, 10ka, 15ka, and 20 ka with three different confidence levels	V	Bentley et al., 2014
	Blue ice areas		V	Hui et al., 2014
	Ice rises inventory		V	Matsuoka et al., 2015
	Subglacial lakes ->			
		Subglacial lakes, Wright & Siegert	V	Wright and Siegert, 2012
		Subglacial lakes, Blankenship	V	Carter et al., 2007
		Subglacial lakes, Smith	V	Smith et al., 2009
		Recovery Subglacial Lakes	V	Bell et al., 2007
		Vostok Subglacial Lake	V	Studinger et al., 2003
	GSFC Drainage systems		V	Rignot et al., 2013
	MEaSUREs Antarctic boundaries (v2)	sub layers for Coastline, Grounding line and Ice boundaries	V	Rignot et al., 2013
	Subglacial water flux (modelled)		R, 1 km	Le Brocq et al., 2013
	ALBMAP compilation ->			Le Brocq et al., 2010
		ALBMAP mask layers for (1) surface topography, (2) bed/bathymetry source, (3) ice free/ice stream, (4) ice plain, and (5) MOA grounidng line	R, 5km	
		ALBMAP Snow accumulation, Arthern	R, 5km	Arthern et al., 2006
		ALBMAP Snow accumulation, Van de Berg	R, 5km	van den Broeke et al., 2006
		ALBMAP Surface air temperature	R, 5km	Comiso, 2000
		ALBMAP Firn thickness (clipped)	R, 5km	van den Broeke, 2008
		ALBMAP Geothermal flux, Fox Maule	R, 5km	Fox-Maule et al., 2005
		ALBMAP Geothermal flux, Shapiro & Ritzwoller	R, 5km	Shapiro and Ritzwoller, 2004
		ALBMAP Upper ice surface elevation	R, 5km	
		ALBMAP Lower ice surface elevation 2	R, 5km	
		ALBMAP Lower ice surface elevation	R, 5km	
		ALBMAP Bed/bathymetry elevation 2	R, 5km	
		ALBMAP Bed/bathymetry elevation	R, 5km	
	MEaSUREs Flow speed ->			Rignot et al., 2011 and Mouginot et al., 2012
		MEaSUREs_Flow vectors	V	
		MEaSUREs Flow speed error	R, 0.45 km	
		MEaSUREs Ice flow speed	R, 0.45 km	
	Firn density ->			Ligtenberg et al., 2011
		Surface firn density (modelled)	R, 33 km	
		Firn depth for density 830 kg/m^3 (modelled)	R, 33 km	
		Firn depth for density 550 kg/m^3 (modelled)	R, 33 km	
	SUMER Ice shelf buttressing (modelled)		R, 1km	Furst et al., 2016
	Surface melt flux (1999-2009, QuikSCAT, observed)		R, 4.5 km	Trusel et al., 2013
Oceanography	Southern Ocean fronts	Sub layers for 5 fronts	V	
	SOSE Mean surface current speed		R, 16 km	Mazloff et al., 2010
	World Ocean Atlas (WOA) 2013 ->			
		Temperature, sub layers for summer and winter at the surface and 50 m, 200 m, and 500 m depths	R, 25 km	Locarnini et al., 2013
		Salinity, sub layers for summer and winter at the surface and 50 m, 200 m, and 500 m depths	R, 25 km	Zweng et al., 2013

(*continued on next page*)

Table 3 (*continued*)

Group	Layer or subgroup	Sub layer or layer description	Data type (Vector or Raster) and spatial resolution if raster	Reference
		Oxygen, sub layers for summer and winter at the surface and 50 m, 200 m, and 500 m depths	R, 25 km	Garcia et al., 2014a
		Silicate, sub layers for summer and winter at the surface and 50 m, 200 m, and 500 m depths	R, 25 km	Garcia et al., 2014b
		Phosphate, sub layers for summer and winter at the surface and 50 m, 200 m, and 500 m depths	R, 25 km	Garcia et al., 2014b
		Nox, sub layers for summer and winter at the surface and 50 m, 200 m, and 500 m depths	R, 25 km	Garcia et al., 2014b
Sea ice	Median sea ice extent 1981-2010	Sub layers for each month	V	Fetterer et al., 2017
	NSIDC Concentration ->			Fetterer et al., 2016
		February (min extent) median between 1981 and 2010	V	
		Sub layers of February (min extent) for eac year from 2007 to 2017	R, 25 km	
		September (max extent) median between 1981 and 2010	V	
		Sub layers of September (max extent) for each year from 2007 to 2017	R, 25 km	
	Proportion of year ice covered		R, 6.25 km	Spreen et al., 2008
Social science	Non-native species incursions		V	Hughes and Pertierra, 2016
	ADD Historic sites and monuments		V	
	Historic stations		V	Headland, 2009
	Historic expedition routes	Sub layers for six expeditions	V	Dater, 1975
Terrain models	BEDMAP2 ->			Fretwell et al., 2013
		BEDMAP2 Data coverage	R, 1 km	
		BEDMAP2 Exposed rock mask	R, 1 km	
		BEDMAP2 Lake Vostok mask	R, 1 km	
		BEDMAP2 Ice outline mask	R, 1 km	
		BEDMAP2 Surface elevation, virtual hillshade	R, 1 km	
		BEDMAP2 Surface elevation	R, 1 km	
		BEDMAP2 Bed elevation, virtual hillshade	R, 1 km	
		BEDMAP2 Bed uncertainty	R, 1 km	
		BEDMAP2 Bed elevation	R, 1 km	
		BEDMAP2 Ice thickness uncertainty	R, 1 km	
		BEDMAP2 Ice thickness	R, 1 km	
	ADD Contours	High spatial resolutions, variable intervals	V	
	ADD Contours	low resolution, 1000-m interval	V	
	RAMP2 Contours	100 m and customizable interval	V	Liu et al., 2015
	RAMP2 OSU Contours	100 m and customizable interval	V	Liu et al., 2015
	RAMP2 Elevation model		R, 0.2 km	Liu et al., 2015
	RAMP2 Elevation model, hillshade		R, 0.2 km	Liu et al., 2015
	RAMP2 Elevation model (OSU91a datum)		R, 0.2 km	Liu et al., 2015
	CryoSat-2 Contours	100 m and customizable intervals	V	Helm et al., 2014
	CryoSat-2 Elevation model error		R, 1 km	Helm et al., 2014
	CryoSat-2 Elevation model		R, 1 km	Helm et al., 2014
	CryoSat-2 Elevation model, hillshade		R, 1 km	Helm et al., 2014
	IBCSO Contours	1000 m intervals	V	Arndt et al., 2013
	IBCSO Data type		R, 0.5 km	Arndt et al., 2013
	IBCSO Elevation model, surface		R, 0.5 km	Arndt et al., 2013
	IBCSO Elevation model, surface, hillshade		R, 0.5 km	Arndt et al., 2013
	IBCSO Elevation model, bed		R, 0.5 km	Arndt et al., 2013
	IBCSO Elevation model, bed, hillshade		R, 0.5 km	Arndt et al., 2013
	ETOPO1 Contours	1000 m intervals	V	NOAA National Geophysical Data Center (2009)
	ETOPO1 Elevation model		R, 2km	NOAA National Geophysical Data Center (2009)
	ETOPO1 Elevation model, hillshade		R, 2km	NOAA National Geophysical Data Center (2009)
Satellite imagery	Landsat subantarctic index		V R, 15 m	

(*continued on next page*)

Table 3 (*continued*)

Group	Layer or subgroup	Sub layer or layer description	Data type (Vector or Raster) and spatial resolution if raster	Reference
	USGS/NASA subantarctic Landsat			
	LIMA Landsat high-resolution tiles index		V	Bindschadler et al., 2008
	LIMA Landsat high-resolution virtual mosaic		R, 15 m	Bindschadler et al., 2008
	LIMA Landsat low-resolution mosaic		R, 240 m	Bindschadler et al., 2008
	MODIS mosaic		R, 125 m	Haran et al., 2014; Scambos et al., 2007
	RAMP RADARSAT mosaic		R, 100 m	Jezek et al., 2013
Detailed basemap	RAMP2 Hillshade	Regular and 2x v. exag	R, 200 m	Liu et al., 2015
	ADD Coastlines	High and low resolution	V	
	ADD Streams	High resolution	V	
	ADD Lakes (high)	High and medium resolution	V	
	ADD Contours	High, medium and low resolution	V	
	ADD Moraines	High and medium resolution	V	
	ADD Rock_outcrop	High, medium and low resolution	V	
	ADD Coastlines	High, medium and low resolution	V	
	ETOPO1/IBCSO/RAMP2 Hillshade	5, 10, 25 and 50 times vertical exaggeration	R, 0.5 - 10 km	NOAA National Geophysical Data Center (2009)
	ADD Simple basemap, Sub-antarctic		V	
	ETOPO1/IBCSO/RAMP2 Elevation model		R, 2 km	Liu et al., 2015; Arndt et al., 2013; NOAA National Geophysical Data Center (2009)
ADD Simple basemap		Ice shelf, Land, Ocean, and Sub-antarctic	V	

3.7. Environmental management data

This discipline focuses on specially designated areas for environmental protection purposes. Included are the Antarctic Specially Protected Areas (ASPAs; Terauds, 2016), and Antarctic Specially Managed Areas (ASMAs; https://www.ats.aq/devph/en/apa-database/search#apa-results) adopted by the Parties to the Antarctic Treaty under the provisions of Annex V to the Protocol on Environmental Protection to the Antarctic Treaty. Also included are the Convention for the Conservation of Antarctic Marine Living Resources' (CCAMLR's) Marine Protected Areas (MPAs), Small-Scale Management Units (SSMUs), and Small-Scale Research Units (SSRUs), all available from https://gis.ccamlr.org/home/ccamlrgis, as well as 16 Antarctic Conservation Biogeographic Regions (ACBRs) that cover most ice-free areas in Antarctica (Terauds et al., 2012; Terauds and Lee, 2016).

3.8. Geology data

Geological data layers include ADD's high-resolution rock outcrop (Burton-Johnson et al., 2016), undersea geomorphic features (Post et al., 2014), a schematic geological map (Tingey, 1991), tectonic plate boundaries (Fig. 2c; Bird, 2003), and epicentres of earthquakes since 1900 (Fig. 2c, https://earthquake.usgs.gov/earthquakes/search/). This discipline has three more layers. The first layer has attributes of the data source at each location of multibeam seafloor survey data included in IBCSO's bathymetry terrain model (Arndt et al., 2013). The second layer is locations of rock and sediment samples available from the Byrd Polar and Climate Research Center's Rock Repository at Ohio State University (https://research.bpcrc.osu.edu/rr/). Users can learn about the sample by clicking a feature and can request a physical sample. The third layer shows the coverage of geological maps used for SCAR's ongoing GeoMAP project to compile numerous geological maps (Cox et al., 2019). These three layers provide additional use to geologists, rather than presenting established knowledge for a wide audience. Nonetheless, these layers are most useful when displayed together with other datasets and act as important tools in QA to explore a diverse array of potential projects.

3.9. Geophysics data

Geophysics data include two gravity-field and one magnetic-field datasets. The first gravity-field one gives 10-km-resolution free-air and Bouguer gravity anomalies. It was developed by the International Association of Geodesy's (IAG) subcommission 2.4f Gravity and Geoid in Antarctica (AntGG) using ground-based, airborne, and shipborne data (Fig. 3a; Scheinert et al., 2016). Above the anomalies, a semi-transparent layer gives the accuracy estimates. As the transparency is assigned in terms of accuracy, anomalies are less visible at lower accuracy. The second one is a satellite-based EIGEN-6C4 gravity field (geoid) model available for 60°S poleward (Förste et al., 2014), which has lower-resolution, yet greater geographical coverage than the AntGG compilation (Fig. 3a). Finally, the magnetic-field dataset is a satellite-measured magnetic field with 5-km resolution for ~59–90°S from SCAR's Antarctic Digital Magnetic Anomaly Project (ADMAP; Golynsky et al., 2013; Golynsky et al., 2001). Also included are magnetic pole locations since 1590 and present-day magnetic declination contours, which may be used in fieldwork (Chulliat et al., 2014). For sub-surface geothermal flux, the geophysics discipline includes one dataset inferred from seismic velocity (An et al., 2015), which adds to the two datasets in glaciology's ALBMAP compilation (Section 3.10).

3.10. Glaciology and ice-core data

Glaciological and ice-core data have the largest data volume in QA3. Data are provided on grounding lines (Bindschadler et al., 2011), hydrostatic lines (Bindschadler et al., 2011), two sets of major drainage boundaries (http://icesat4.gsfc.nasa.gov/cryo_data/ant_grn_drainage_systems.php, and Rignot et al., 2013), and an inventory of coastal ice rises and rumples (Matsuoka et al., 2015), all of which give the basic form of the Antarctic Ice Sheet. For the grounding and hydrostatic lines, colours indicate the level of confidence in their locations. Looking to the past, paleo ice-sheet extents are shown at four epochs since the Last

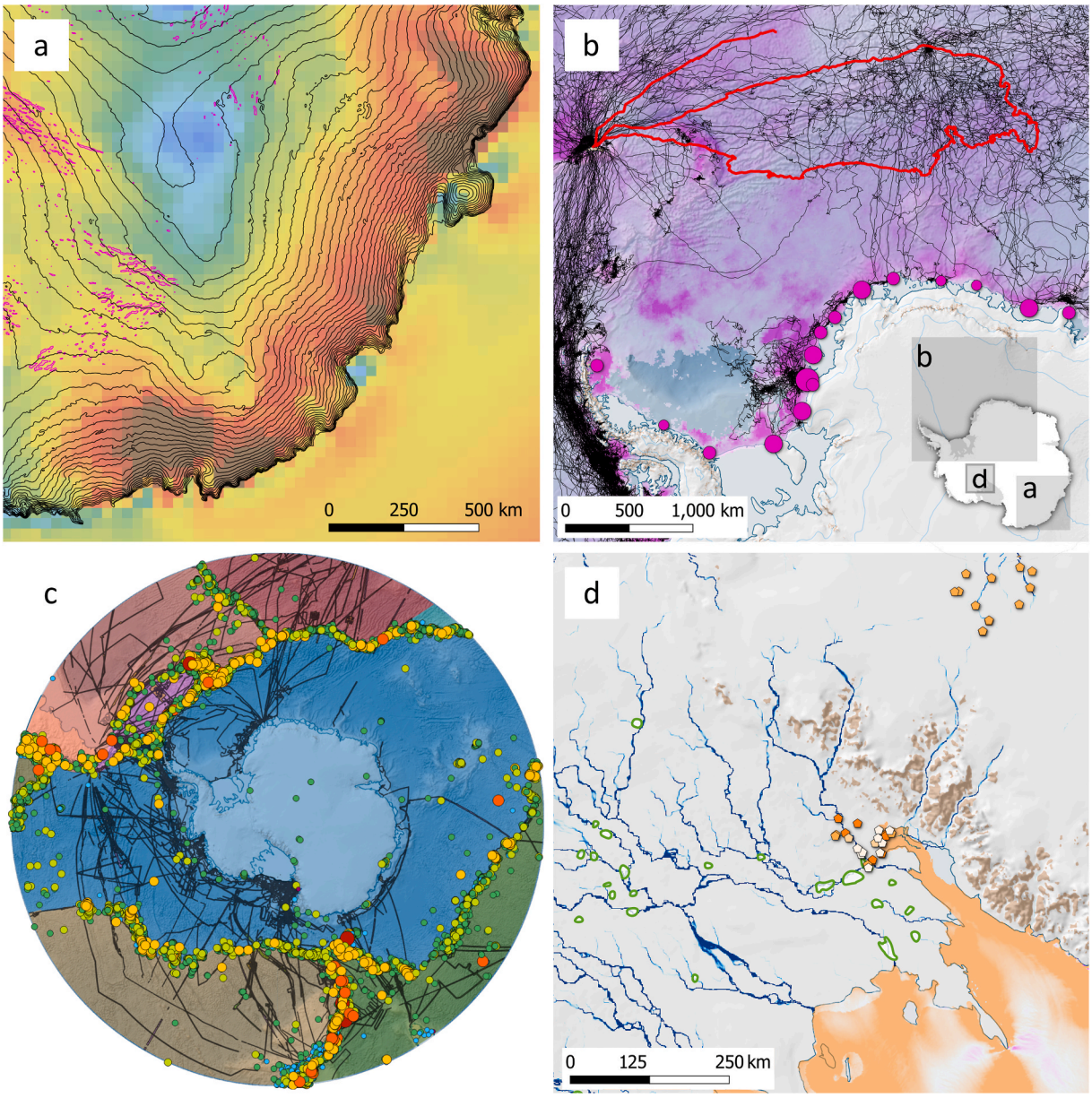

Fig. 2. Quantarctica data visualization examples that involve several disciplines and multiple sources. Inset in panel (b) is the simple basemap showing geographical coverages of panels (a), (b), and (d). Colour bars and legends for each layer appear in the layer panel of the QA workplace (Fig. 1); those and other properties (e.g., grids and north arrow) can be added to these presentations using QGIS's Print Layout function. For simplicity, we show here only the distance bar to (a), (b), and (d). (a) Annual-average, 10-m wind speeds modelled with a regional atmospheric climate model RACMO2 (van Wessem et al., 2014b) and satellite-mapped wind scour zones (Das et al., 2013) are plotted together with CryoSat-2's ice-surface elevation contours (100 m intervals; Helm et al., 2014). (b) MEOP profile locations recorded by loggers equipped to seals (Treasure et al., 2017) and satellite-mapped Emperor penguin colony locations with estimated populations given by the circle sizes (Fretwell et al., 2012) superimposed on chlorophyll-a summer density (Johnson et al., 2017) and detailed basemap. One of 685 MEOP tracks is selected (red) so that one can use QGIS's identify features tool to see attributes of this track (e.g., data collection time, file name for the full dataset, seal platform used for the data collection). (c) Epicentres of earthquakes with colour indicating magnitudes are shown clustered along the tectonic plate boundaries. Thin black curves mark locations of multibeam bathymetry data used for the IBCSO's bathymetry compilation (Arndt et al., 2013). (d) Subglacial lakes outlined (Smith et al., 2009) and shown with different colours for different lake properties (Carter et al., 2007), superimposed on modelled subglacial water flux (blue; Le Brocq et al., 2013) and outcrops (brown) using the detailed basemap. Orange–pink shading at bottom right over the ice shelf is modelled magnitude of buttressing given to the upstream ice (Furst et al., 2016).

Glacial Maximum, together with three levels of confidence (Bentley et al., 2014). A 450-m-resolution surface ice-flow field derived from satellite data is shown in a raster and also as flow vectors (Fig. 3b; Mouginot et al., 2012; Rignot et al., 2011). Flow-speed uncertainty appears in a semi-transparent layer consistent with those given for the gravity layers (Section 3.9). Differential roles of ice shelves in stabilizing the grounding line and inland ice sheet are modelled at the 1-km resolution (Fig. 2d; Furst et al., 2016). Melting at the base of the ice sheet is represented by about 130 satellite-detected active subglacial lakes, which are filled and drained repeatedly over months to years (Smith et al., 2009), and about 250 radar-detected subglacial lakes (Fig. 2d; Bell et al., 2007; Carter et al., 2007; Studinger et al., 2003; Wright and Siegert, 2012). At some locations, the modelled subglacial water flux (Le Brocq et al., 2013) shows the meltwater network that connects these lakes and drains to the ocean. Other data layers are modelled surface firn density (with depths at which the firn density reaches about 60% and

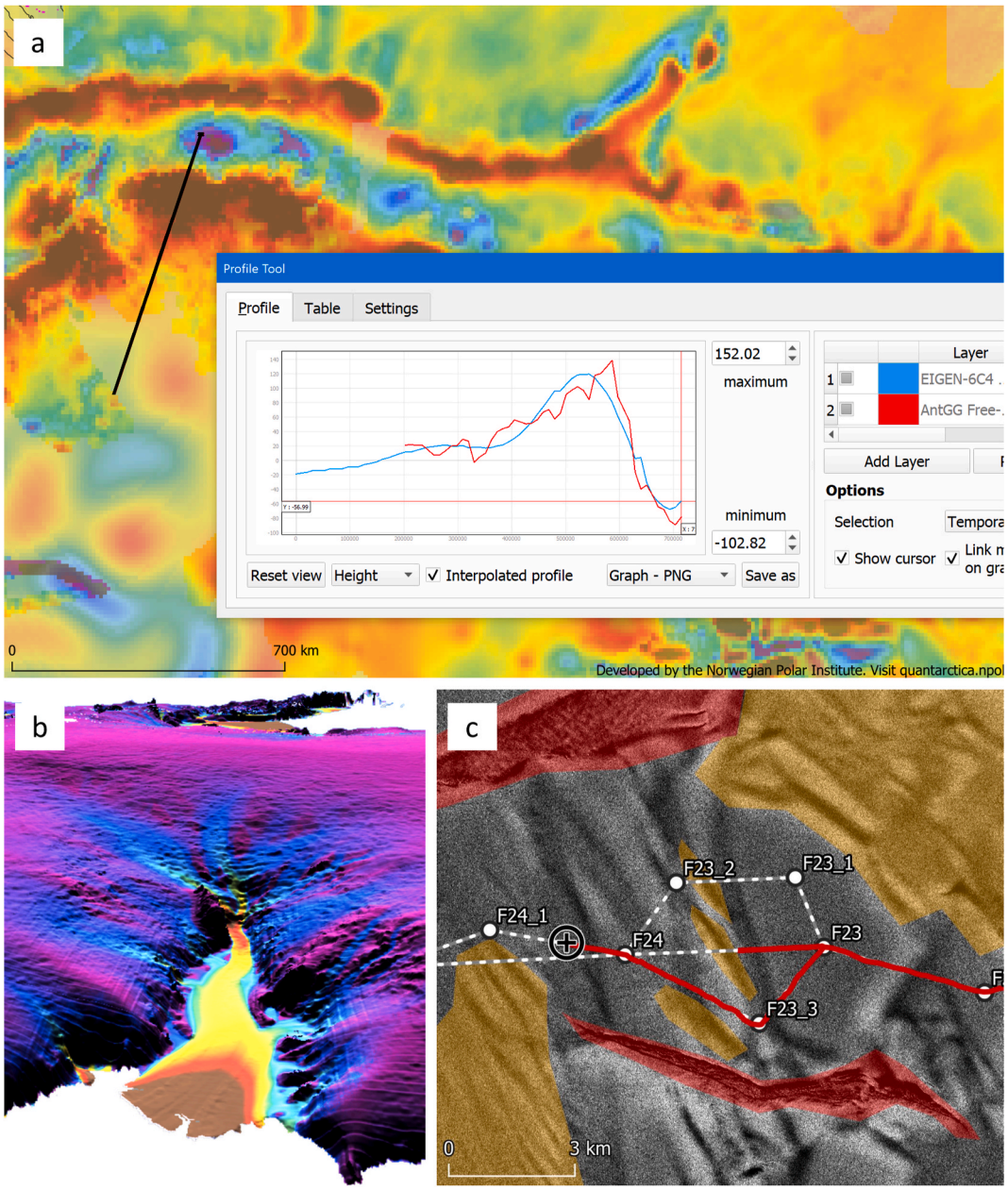

Fig. 3. Sample of Quantarctica applications. (a) QGIS's profile tool shows raster values along the black line (connected line segments can be profiled). For this specific case, the airborne-measured high-resolution AntGG free-air gravity anomaly (Scheinert et al., 2016) is shown together with the satellite-measured low-resolution EIGEN-6C4 gravity disturbance (Förste et al., 2014). (b) QGIS's 3D perspective capability allows users to see glaciers going down the coastal slope towards an ice shelf. Ice-flow speed (Mouginot et al., 2012; Rignot et al., 2011) is shown on the CryoSat-2's ice-surface topography (exaggerated 50 times vertically; Helm et al., 2014). (c) To plan fieldwork, high-resolution satellite imagery (in this case, RADARSAT-2 using snow-penetrating microwave) taken just before the deployment is loaded to QGIS. Darker areas arise from both surface topography and exposed or snow-covered crevasses. Independent analysts worked on this image and developed a group consensus of zoning of hazardous (red) and cautious (yellow-brown), and a few alternative routes with waypoints (white dots). During fieldwork, one can also superimpose the vehicle's trajectory (solid red) and current position (plus mark) obtained by a GPS receiver connected to the navigation laptop. For this case, the first choice of the three routes from the site F23 did not work, so the traverse team returned to the waypoint F23 and made the second choice through F23_3, which was successful. RADARSAT-2 Data and Products copyrighted by MacDonald, Dettwiler and Associates Ltd (2013). All Rights Reserved. RADARSAT is an official mark of the Canadian Space Agency.

90% of the pure-ice density) (Ligtenberg et al., 2011), satellite-observed, 5-km resolution surface melt flux averaged between 1999 and 2009 (Trusel et al., 2013), and satellite-observed blue ice areas (Hui et al., 2014).

ALBMAP is a compilation of glaciological datasets (Le Brocq et al., 2010) that include satellite-observed and modelled surface mass balance (Arthern et al., 2006; van den Broeke et al., 2006), modelled surface temperature (Comiso, 2000) and firn thickness (van den Broeke, 2008), two geothermal flux datasets inferred each from global seismic models (Shapiro and Ritzwoller, 2004) and satellite-measured magnetic fields (Fox-Maule et al., 2005), and newly-generated ice and bed topography datasets. These individual datasets originally have different spatial resolutions, extents, and geographic projections. ALBMAP modifies these original datasets and provides them with 5-km-resolution to be used as boundary conditions for ice-flow modelling. We include ALBMAP in QA as a grouped set of layers.

QA3 has an ice-core database that includes the location, depth, and reported literature of 241 ice cores around Antarctica, which were reported by ITASE IceReader (http://www.icereader.org/icereader/listData.jsp), Climate Change Institute Antarctic Ice Core Data (http://cci.icecoredata.org/Antarctica.html) and WAIS Divide Ice Core Project (Fudge et al., 2013). Also included is a dataset of surface mass balance measured at 3236 sites, together with metadata for each site showing methods, and the year of ice-core retrieval (Favier et al., 2013). This measured surface mass balance dataset complements model output layers included in the atmosphere discipline (Section 3.5). Isotopic compositions of snow, with a complete attribute table, are reported at 1279 locations, which are presented using progressive symbol colours for $\delta^{18}O$ of water stable isotope ratios, a proxy for the local temperature (Touzeau et al., 2016).

3.11. Oceanography data

QA3 includes oceanography data to 40°S, so that the Subantarctic Ocean Front and even most of the Subtropical Ocean Front are included. Most oceanography data layers are taken from the World Ocean Atlas 2013 (WOA), including temperature (Locarnini et al., 2013), salinity (Zweng et al., 2013), and concentrations of oxygen (Garcia et al., 2014a), silicate, phosphate, and nitrate (Garcia et al., 2014b) at the surface and three depths (50, 200, and 500 m), both in the summer and winter (Fig. 1). All WOA data layers are gridded every 25 km. Other oceanography datasets include five ocean fronts (Southern Antarctic Circumpolar Current Front, Southern Boundary of the Antarctic Circumpolar Current, Polar Front, Subantarctic Front, and Subtropical Front), and a grid of mean surface current speed with the 16-km resolution that is obtained using observation-data assimilation techniques (Mazloff et al., 2010).

3.12. Sea ice data

For sea ice data, QA3 has satellite-observed, monthly median sea ice extent between 1981 and 2010 (Fetterer et al., 2017). To indicate historical changes and seasonal variability, satellite-observed, 25-km resolution sea ice concentrations in September (maximum coverage in early austral summer) and February (minimum coverage) are included for each year from 2007 to 2017 (Fetterer et al., 2016). The proportion of time the ocean is covered by sea ice with a concentration of 85% or higher is mapped at 6-km resolution using satellite data from 2002 to 2011 (Spreen et al., 2008).

3.13. Social sciences data

Data here include human footprints in Antarctica since the early stage of expeditions. Routes and tracks of six historic Antarctic expeditions are presented, including the first circumnavigation of Antarctica by Fabian Gottlieb von Bellingshausen in 1819–1821, tracks to the South Pole by Roald Amundsen and Robert Falcon Scott in early 1910s, and the first trans-Antarctic flight by Lincoln Ellsworth in 1935 (Dater, 1975). Historic stations (Headland, 2009) as well as historic sites and monuments included in ADD are presented. These include 103 stations on the continent and 36 more on surrounding islands developed by 24 nations between the first International Polar Year 1882–1883 and its fourth one in 2007–2009. Human activities in Antarctica have increased dramatically in recent decades through research, expeditions, and tourism. Consequently, non-native species were brought to terrestrial Antarctica; locations and brief descriptions of 39 documented biological invasion cases in terrestrial Antarctica are presented here (Hughes and Pertierra, 2016).

4. Discussion

4.1. User applications

Quantarctica is a multidisciplinary knowledge base for Antarctica, the Southern Ocean, and sub-Antarctic islands. It has given researchers, students, educators, and logistics operators a single, easy-to-use platform to view, analyse, and synthesize Antarctic datasets (Perkel, 2018). QA3 is distributed with the CC-BY4.0 license, so users can develop their own GIS environment using QA as its basis, and visually present their own data with QA as the graphical basis in many scientific publications over various disciplines, such as Quaternary science (Andersen et al., 2020), oceanography (Schiaparelli and Aliani, 2019), behavioural ecology (Schiaparelli and Aliani, 2019), and microorganisms (Hirose et al., 2020). Cautions are needed, however, because some datasets have different licenses, terms of use, and attribution requirements, which are documented in the metadata. QA can be freely distributed and thus it is hard to know the actual number of users, but we know of users from all SCAR member countries, including those currently in the early stages of developing full-scale Antarctic programs. The SCAR Expert Group on Antarctic Biodiversity Informatics has developed a R package quantarcticR (https://github.com/SCAR/quantarcticR) that provides access to QA datasets for R users, without needing QGIS to be installed. With the success of QA, a similar GIS data package is being developed for the Greenland Ice Sheet (QGreenland, https://qgreenland.org/).

Many users import non-QA datasets to develop their own GIS workspaces based on QA. QGIS provides numerous tools and plugins to help analyse QA datasets. The identify features tool provides detailed information on selected vector data points (e.g., red profile in Fig. 2b) or cell values of selected raster layers. The attribute tables list information that can be sorted or filtered by field properties. Some commonly used analytical tools include polygonization of raster/vector datasets, contour extractions, terrain (slope and aspect) analysis, and raster calculation using multiple scientific datasets and terrain models, as well as interpolation, smoothing, and merging of multiple raster datasets (e.g., continental data in QA and user's own data in a smaller region). The profile tool displays the transect of raster values along custom line segments (Fig. 3a). QGIS also allows 3D viewing (Fig. 3b). Selected datasets can be draped over three-dimensional representations of a terrain model with various angles and vertical exaggerations. QGIS has many other tools and plugins.

Due to its modest computational requirements, QA can be easily used on laptops during Antarctic fieldwork. Before deploying to the field, QA's data layers, satellite imagery and basemaps can be used for the first-order safety assessments. In addition, users can import recent satellite imagery and analyse them on the QA workspace to define hazardous crevasse areas and design traverse routes (Fig. 3c). QGIS also works to plot the user's current location using a handheld GPS receiver. This capability increases safety and speed during field traverses. During fieldwork, researchers can gain a deeper understanding of a region by displaying QA's included package of scientific data and satellite imagery.

4.2. Quantarctica-friendly datasets

The number of data layers and the data volume in the QA package are limited to those with a large spatial coverage and useful for multidisciplinary users, so that users can easily browse data outside of their own disciplines. However, individual users working in a specific region or specific discipline need more detailed data. To improve user experience and promote data sharing, we encourage data providers to follow our recommendations and mandatory guidelines (ftp://ftp.quantarctica.npolar.no/Quantarctica3/Making%20Quantarctica-friendly%20datasets.pdf). Those datasets that meet these criteria, called Quantarctica-friendly datasets, are hosted by the data providers, and download links and short descriptions are listed at QA's project web site (https:

//www.npolar.no/quantarctica/).

Mandatory guidelines are file formats (ESRI shapefile for vector and GeoTIFF, or if needed JPEG2000 or JPEG, for raster), layer style file (.QML format), metadata file (.QMD format and TXT file with only the meta data abstract for convenience and clarity), and projection (EPSG:3031). Also, we recommend the following: (1) specific layer styles and labelling to visualize the data compatible with QA's datasets, (2) image pyramids of large raster data for faster rendering, and (3) raster data compression, preferably using lossless LZW or Deflate compression, but also if needed using lossy compression such as JPEG2000 for large-volume data. Datasets currently listed as Quantarctica-friendly datasets include region-specific bed topography data in the Weddell Sea (Jeofry et al., 2018), electronic navigational chart coverage and tide records as a part of GIS service maintained by the Hydrographic Commission of Antarctica under the International Hydrographic Organization (https://data-iho.opendata.arcgis.com/), and modelled permafrost temperature validated with observations in 2000–2017 (Obu et al., 2020).

4.3. QGIS functionality in polar regions

In our development of QA, we contributed to the development of the following three functions of QGIS that benefit QA users as well as QGIS users in the Arctic. (1) Print Layout can now display the north arrow pointing to true north (not to the grid north) in polar coordinate systems (https://www.qgis.org/en/site/forusers/visualchangelog218/index.html#feature-true-north-arrows). This is particularly useful in maps of small regions. (2) QGIS can now render, select, and edit on-the-fly projected vector data when on-the-fly reprojection is enabled for EPSG:3031 and other polar stereographic projections (https://issues.qgis.org/issues/7596#change-64937). This problem occurred when users loaded their own data not projected to EPSG:3031 to QA's workplace as a test before re-projecting their data to EPSG:3031. (3) The GarminCustomMap plugin is now ported from QGIS2 to QGIS3 (https://plugins.qgis.org/plugins/GarminCustomMap/version/3.0/). This plugin enables the user to export what is visible on the map canvas in QGIS, as a raster image file to the KMZ file format, which can be loaded on most modern Garmin handheld GPS units. This function is commonly used during fieldwork.

4.4. Outlook

The scientific disciplines included in QA are not comprehensive. For example, data for upper atmosphere research and astronomy are absent in the current version, as are Antarctic Ice Sheet mass balance estimates and trends. As new datasets with higher precision and resolution become available, adding new datasets and replacing obsolete datasets are necessary to provide a state-of-the-art knowledge base to the entire Antarctic and Southern Ocean community. We seek to maintain QA as a balanced product in terms of portability, coverage, and user friendliness.

5. Conclusions

Quantarctica (https://www.npolar.no/quantarctica) is an integrated mapping environment for Antarctica, the Southern Ocean, and sub-Antarctic islands, freely available with the CC-BY4.0 license with DOI: https://doi.org/10.21334/npolar.2018.8516e961. Quantarctica works with QGIS software version 3.16 on multiple platforms without an internet connection. It is composed of 265 data layers in simple and detailed basemaps, satellite imagery, terrain models, and scientific data in nine disciplines of atmosphere, biology, environment management, geology, geophysics, glaciology and ice cores, oceanography, sea ice and social science, giving the total data size of 7.53 GB. We will maintain Quantarctica by adding new datasets and replacing obsolete datasets to provide a state-of-the-art knowledge base in a balanced form in terms of portability, coverage, and user friendliness.

Author contributions

Kenichi Matsuoka and Anders Skoglund co-founded Quantarctica and have led its development from the beginning. George Roth was a project coordinator for QA version 3. Assistance with the development of other versions was provided by Angela von Deschwanden (version 1), César Deschamps-Berger (version 2), and Brice Van Liefferinge (version 3.2). Stein Tronstad and Yngve Melvær promoted synergies with SCAR's Data Management Committee (SCADM) and SCAR's Geographic Information (SCAGI), respectively. The other authors are editorial board members for version 3, acting to recommend scientific data for each discipline, and enhancing the overall quality of the product: Jean de Pomereu (social science), Huw Griffiths (biology), Robert Headland (social science), Brad Herried (miscellaneous base layers), Katsuro Katsumata (oceanography), Anne Le Brocq (glaciology), Kathy Licht (geology), Fraser Morgan (environment management), Peter D. Neff (ice cores), Catherine Ritz (glaciology), Mirko Scheinert (geophysics), Takeshi Tamura (sea ice), Anton Van de Putte (biology), and Michiel van den Broeke (atmospheric science). All authors (except for the deceased Angela von Deschwanden) contributed to the development of this paper.

Declaration of competing interest

The authors declare that they have no known competing financial interests or personal relationships that could have appeared to influence the work reported in this paper.

Acknowledgements

Development of Quantarctica version 3 was funded by the Norwegian Ministry of Foreign Affairs (grant number: QZA-15/0332). Quantarctica became highly visible and widely used in the Antarctic community, thanks to SCAR's endorsement of QA as a SCAR product and promotions made by Association of Polar Early Career Scientists (APECS), and SCAR's scientific research programs, action groups and expert groups, as well as SCADM and SCAGI. The Norwegian Environment Agency, Tasmanian Partnership for Advanced Computing, Arctic and Antarctic Data Archive System at the National Institute of Polar Research, National Center for Polar and Ocean Research, and Polar Geospatial Center provide distributed global download capabilities. The RADARSAT-2 image used in Fig. 3c provided by NSC/KSAT under the Norwegian-Canadian RADARSAT agreement. We acknowledge all data providers who supported Quantarctica.

References

An, M.J., Wiens, D.A., Zhao, Y., Feng, M., Nyblade, A., Kanao, M., Li, Y.S., Maggi, A., Leveque, J.J., 2015. Temperature, lithosphere-asthenosphere boundary, and heat flux beneath the Antarctic Plate inferred from seismic velocities. J. Geophys. Res. Solid Earth 120 (12), 8720–8742.

Andersen, J.L., Newall, J.C., Blomdin, R., Sams, S.E., Fabel, D., Koester, A.J., Lifton, N.A., Fredin, O., Caffee, M.W., Glasser, N.F., Rogozhina, I., Suganuma, Y., Harbor, J.M., Stroeven, A.P., 2020. Ice surface changes during recent glacial cycles along the Jutulstraumen and Penck Trough ice streams in western Dronning Maud Land, East Antarctica. Quat. Sci. Rev. 249, 106636.

Arndt, J.E., Schenke, H.W., Jakobsson, M., Nitsche, F.O., Buys, G., Goleby, B., Rebesco, M., Bohoyo, F., Hong, J., Black, J., Greku, R., Udintsev, G., Barrios, F., Reynoso-Peralta, W., Taisei, M., Wigley, R., 2013. The International Bathymetric Chart of the Southern Ocean (IBCSO) Version 1.0 – a new bathymetric compilation covering circum-Antarctic waters. Geophys. Res. Lett. 40, 3111–3117.

Arthern, R.J., Winebrenner, D.P., Vaughan, D.G., 2006. Antarctic snow accumulation mapped using polarization of 4.3-cm wavelength microwave emission. J. Geophys. Res. Atmos. 111 (D6), D06107.

Atkinson, A., Hill, S.L., Pakhomov, E.A., Siegel, V., Anadon, R., Chiba, S., Daly, K.L., Downie, R., Fielding, S., Fretwell, P., Gerrish, L., Hosie, G., Jessopp, M.J., Kawaguchi, S., Krafft, B.A., Loeb, V., Nishikawa, J., Peat, H.J., Reiss, C.S., Ross, R.M., Quetin, L.B., Schmidt, K., Steinberg, D.K., Subramaniam, R.C., Tarling, G.A., Ward, P., 2017. KRILLBASE: a circumpolar database of Antarctic krill and salp numerical densities, 1926-2016. Earth Syst. Sci. Data 9 (1), 193–210.

Bell, R.E., Studinger, M., Shuman, C.A., Fahnestock, M.A., Joughin, I., 2007. Large subglacial lakes in East Antarctica at the onset of fast-flowing ice streams. Nature 445 (7130), 904–907.

Bentley, M.J., Cofaigh, C.O., Anderson, J.B., Conway, H., Davies, B., Graham, A.G.C., Hillenbrand, C.-D., Hodgson, D.A., Jamieson, S.S.R., Larter, R.D., Mackintosh, A., Smith, J.A., Verleyen, E., Ackert, R.P., Bart, P.J., Berg, S., Brunstein, D., Canals, M., Colhoun, E.A., Crosta, X., Dickens, W.A., Domack, E., Dowdeswell, J.A., Dunbar, R., Ehrmann, W., Evans, J., Favier, V., Fink, D., Fogwill, C.J., Glasser, N.F., Gohl, K., Golledge, N.R., Goodwin, I., Gore, D.B., Greenwood, S.L., Hall, B.L., Hall, K., Hedding, D.W., Hein, A.S., Hocking, E.P., Jakobsson, M., Johnson, J.S., Jomelli, V., Jones, R.S., Klages, J.P., Kristoffersen, Y., Kuhn, G., Leventer, A., Licht, K., Lilly, K., Lindow, J., Livingstone, S.J., Masse, G., McGlone, M.S., McKay, R.M., Melles, M., Miura, H., Mulvaney, R., Nel, W., Nitsche, F.O., O'Brien, P.E., Post, A.L., Roberts, S. J., Saunders, K.M., Selkirk, P.M., Simms, A.R., Spiegel, C., Stolldorf, T.D., Sugden, D. E., van der Putten, N., van Ommen, T., Verfaillie, D., Vyverman, W., Wagner, B., White, D.A., Witus, A.E., Zwartz, D., Consortium, R., 2014. A community-based geological reconstruction of Antarctic ice sheet deglaciation since the Last glacial maximum. Quat. Sci. Rev. 100, 1–9.

Bindschadler, R., Choi, H., Wichlacz, A., Bingham, R., Bohlander, J., Brunt, K., Corr, H., Drews, R., Fricker, H., Hall, M., Hindmarsh, R., Kohler, J., Padman, L., Rack, W., Rotschky, G., Urbini, S., Vornberger, P., Young, N., 2011. Getting around Antarctica: new high-resolution mappings of the grounded and freely-floating boundaries of the Antarctic ice sheet created for the International Polar Year. Cryosphere 5 (3), 569–588.

Bindschadler, R., Vornberger, P., Fleming, A., Fox, A., Mullins, J., Binnie, D., Paulsen, S. J., Granneman, B., Gorodetzky, D., 2008. The Landsat image mosaic of Antarctica. Remote Sens. Environ. 112 (12), 4214–4226.

Bird, P., 2003. An updated digital model of plate boundaries. Geochem. Geophys. Geosyst. 4 https://doi.org/10.1029/2001gc000252.

Burton-Johnson, A., Black, M., Fretwell, P.T., Kaluza-Gilbert, J., 2016. An automated methodology for differentiating rock from snow, clouds and sea in Antarctica from Landsat 8 imagery: a new rock outcrop map and area estimation for the entire Antarctic continent. Cryosphere 10, 1665–1677. https://doi.org/10.5194/tc-10-1665-2016.

Carter, S.P., Blankenship, D.D., Peters, M.E., Young, D.A., Holt, J.W., Morse, D.L., 2007. Radar-based subglacial lake classification in Antarctica. Geochem. Geophys. Geosyst. 8 https://doi.org/10.1029/2006gc001408.

Chulliat, A., Macmillan, S., Alken, P., Beggan, C., Nair, M., Hamilton, B., Woods, A., Ridley, V., Maus, S., Thomson, A., 2014. Magnetic Declination Degree Lines and Magnetic South Pole Locations. https://doi.org/10.7289/V5TH8JNW.

Comiso, J.C., 2000. Variability and trends in Antarctic surface temperatures from in situ and satellite infrared measurements. J. Clim. 13 (10), 1674–1696.

Cox, S.C., Smith Lyttle, B., the GeoMAP team, 2019. SCAR GeoMAP dataset. GNS Science, Lower Hutt, New Zealand. https://doi.org/10.21420/7SH7-6K05. Release v.201907.

Das, I., Bell, R.E., Scambos, T.A., Wolovick, M., Creyts, T.T., Studinger, M., Frearson, N., Nicolas, J.P., Lenaerts, J.T.M., van den Broeke, M.R., 2013. Influence of persistent wind scour on the surface mass balance of Antarctica. Nat. Geosci. 6 (5), 367–371.

Dater, Henry M., 1975. History of Antarctic Exploration and Scientific Investigation. In: Bushnell, Vivian C. (Ed.). American Geographical Society.

Douglass, L.L., Turner, J., Grantham, H.S., Kaiser, S., Constable, A., Nicoll, R., Raymond, B., Post, A., Brandt, A., Beaver, D., 2014. A hierarchical classification of benthic biodiversity and assessment of protected areas in the Southern Ocean. PloS One 9 (7), e100551.

Favier, V., Agosta, C., Parouty, S., Durand, G., Delaygue, G., Gallée, H., Drouet, A.S., Trouvilliez, A., Krinner, G., 2013. An updated and quality controlled surface mass balance dataset for Antarctica. Cryosphere 7 (2), 583–597.

Fetterer, F., Knowles, K., Meier, W.N., Savoie, M., Windnagel, A.K., 2016. Updated Daily. Sea Ice Index, Version 2. http://dx.doi.org/10.7265/N5736NV7.

Fetterer, F., Knowles, K., Meier, W.N., Savoie, M., Windnagel, A.K., 2017. Updated Daily. Sea Ice Index, Version 3. https://doi.org/10.7265/N5K072F8.

Fox-Maule, C., Purucker, M.E., Olsen, N., Mosegaard, K., 2005. Heat flux anomalies in Antarctica revealed by satellite magnetic data. Science 309 (5733), 464–467.

Fretwell, P., Pritchard, H.D., Vaughan, D.G., Bamber, J.L., Barrand, N.E., Bell, R., Bianchi, C., Bingham, R.G., Blankenship, D.D., Casassa, G., Catania, G., Callens, D., Conway, H., Cook, A.J., Corr, H.F.J., Damaske, D., Damm, V., Ferraccioli, F., Forsberg, R., Fujita, S., Gim, Y., Gogineni, P., Griggs, J.A., Hindmarsh, R.C.A., Holmlund, P., Holt, J.W., Jacobel, R.W., Jenkins, A., Jokat, W., Jordan, T., King, E. C., Kohler, J., Krabill, W., Riger-Kusk, M., Langley, K.A., Leitchenkov, G., Leuschen, C., Luyendyk, B.P., Matsuoka, K., Mouginot, J., Nitsche, F.O., Nogi, Y., Nost, O.A., Popov, S.V., Rignot, E., Rippin, D.M., Rivera, A., Roberts, J., Ross, N., Siegert, M.J., Smith, A.M., Steinhage, D., Studinger, M., Sun, B., Tinto, B.K., Welch, B.C., Wilson, D., Young, D.A., Xiangbin, C., Zirizzotti, A., 2013. Bedmap2: improved ice bed, surface and thickness datasets for Antarctica. Cryosphere 7 (1), 375–393.

Fretwell, P.T., LaRue, M.A., Morin, P., Kooyman, G.L., Wienecke, B., Ratcliffe, N., Fox, A. J., Fleming, A.H., Porter, C., Trathan, P.N., 2012. An emperor penguin population estimate: the first global, synoptic survey of a species from Space. PloS One 7 (4).

Fudge, T.J., Steig, Eric J., Markle, Bradley R., Schoenemann, Spruce W., Ding, Qinghua, Taylor, Kendrick C., McConnell, Joseph R., Brook, Edward J., Sowers, Todd, White, James W.C., Alley, Richard B., Cheng, Hai, Clow, Gary D., Cole-Dai, Jihong, Conway, Howard, Cuffey, Kurt M., Edwards, Jon S., Lawrence Edwards, R., Edwards, Ross, Fegyveresi, John M., Ferris, David, Fitzpatrick, Joan J., Johnson, Jay, Hargreaves, Geoffrey, Lee, James E., Maselli, Olivia J., Mason, William, McGwire, Kenneth C., Mitchell, Logan E., Mortensen, Nicolai, Neff, Peter, Anais, J., Orsi, Trevor J. Popp, Schauer, Andrew J., Severinghaus, Jeffrey P., Michael Sigl, Spencer, Matthew K., Vaughn, Bruce H., Voigt, Donald E., Waddington, Edwin D., Wang, Xianfeng, Wong, Gifford J., 2013. Onset of deglacial warming in West Antarctica driven by local orbital forcing. Nature 500, 440–444.

Furst, J.J., Durand, G., Gillet-Chaulet, F., Tavard, L., Rankl, M., Braun, M., Gagliardini, O., 2016. The safety band of Antarctic ice shelves. Nat. Clim. Change 6, 479–482.

Förste, C., Bruinsma, S.L., Abrikosov, O., Lemoine, J.-M., Marty, J.C., Flechtner, F., Balmino, G., Barthelmes, F., Biancale, R., 2014. EIGEN-6C4 the Latest Combined Global Gravity Field Model Including GOCE Data up to Degree and Order 2190 of GFZ Potsdam and GRGS Toulouse.

Garcia, Hernan E., Boyer, Timothy P., Locarnini, Ricardo A., Antonov, John I., Mishonov, Alexey V., Baranova, Olga K., Zweng, Melissa M., Reagan, James R., Johnson, Daphne R., 2013. WORLD OCEAN ATLAS 2013 Volume 3: Dissolved Oxygen, Apparent Oxygen Utilization, and Oxygen Saturation. In: Levitus, S., Mishonov Technical, A. (Eds.), NOAA Atlas NESDIS, vol. 75, p. 35. https://doi.org/10.7289/V5XG9P2W. https://repository.library.noaa.gov/view/noaa/14849.

Garcia, Hernan E., Locarnini, Ricardo A., Boyer, Timothy P., Antonov, John I., Baranova, Olga K., Zweng, Melissa M., Reagan, James R., Johnson, Daphne R., 2013. WORLD OCEAN ATLAS 2013 Volume 4: Dissolved Inorganic Nutrients (phosphate, nitrate, silicate). In: Levitus, S., Mishonov Technical, A. (Eds.), NOAA Atlas NESDIS, vol. 76, p. 33. https://doi.org/10.7289/V5J67DWD. https://repository.library.noaa.gov/view/noaa/14850.

Golynsky, A., Bell, R., Blankenship, D., Damaske, D., Ferraccioli, F., Finn, C., Golynsky, D., Ivanov, S., Jokat, W., Masolov, V., Riedel, S., von Frese, R., Young, D., Grp, A.W., 2013. Air and shipborne magnetic surveys of the Antarctic into the 21st century. Tectonophysics 585, 3–12.

Golynsky, A., Chiappini, M., Damaske, D., Ferraccioli, F., Ferris, J., Finn, C., Ghidella, M., Isihara, T., Johnson, A., Kim, H.R., Kovacs, L., LaBrecque, J., Masolov, V., Nogi, Y., Purucker, M., Taylor, P., Torta, M., 2001. Admap – magnetic anomaly map of the Antarctic, 1:10 000 000 scale map. In: Morris, P., von Frese, R. (Eds.), Brith Antarctic Survey Miscellaneous Map Series, 10. British Antarctic Survey, Cambridge.

Greene, C.A., Gwyther, D.E., Blankenship, D.D., 2017. Antarctic mapping tools for Matlab. Comput. Geosci. 104, 151–157.

Haran, T., Bohlander, J., Scambos, T., Painter, T., Fahnestock, M., 2014. MODIS Mosaic of Antarctica 2008-2009 (MOA2009) Image Map. National Snow and Ice Data Center. http://dx.doi.org/10.7265/N5KP8037.

Harris, C., Fishpool, L., Lascelles, B., Lorenz, K., 2016. Important Bird Areas in Antarctica. Antarctic Environments Portal. https://doi.org/10.18124/D40594.

Headland, R.K., 2009. Antarctic winter scientific stations to the international polar year, 2007–2009. Polar Rec. 45 (1), 9–24.

Helm, V., Humbert, A., Miller, H., 2014. Elevation and elevation change of Greenland and Antarctica derived from CryoSat-2. Cryosphere 8 (4), 1539–1559.

Hirose, Y., Shiozaki, T., Otani, M., Kudoh, S., Imura, S., Eki, T., Harada, N., 2020. Investigating algal communities in lacustrine and hydro-terrestrial environments of East Antarctica using deep amplicon sequencing. Microorganisms 8 (4).

Hughes, K.A., Pertierra, L.R., 2016. Evaluation of non-native species policy development and implementation within the Antarctic Treaty area. Biol. Conserv. 200, 149–159.

Hui, F., Ci, T., Cheng, X., Scambo, T.A., Liu, Y., Zhang, Y., Chi, Z., Huang, H., Wang, X., Wang, F., Zhao, C., Jin, Z., Wang, K., 2014. Mapping blue-ice areas in Antarctica using ETM+ and MODIS data. Ann. Glaciol. 55 (66), 129–137.

Jeofry, H., Ross, N., Corr, H.F.J., Li, J., Morlighem, M., Gogineni, P., Siegert, M.J., 2018. A new bed elevation model for the Weddell Sea sector of the west Antarctic ice sheet. Earth Syst. Sci. Data 10 (2), 711–725.

Jezek, K.C., Curlander, J.C., Carsey, F., Wales, C., Barry, R.G., 2013. RAMP AMM-1 SAR Image Mosaic of Antarctica, Version 2. NASA National Snow and Ice Data Center Distributed Active Archive Center, Boulder, Colorado USA. https://doi.org/10.5067/8AF4ZRPULS4H.

Johnson, R., Strutton, P.G., Wright, S.W., McMinn, A., Meiners, K.M., 2013. Three improved satellite chlorophyll algorithms for the Southern Ocean. J. Geophys. Res.: Oceans 118 (7), 3694–3703.

Johnson, R., Sumner, M., Raymond, B., 2017. Southern Ocean Summer Chlorophyll-A Climatology. Australian Antarctic Data Centre. https://doi.org/10.4225/15/5906b48f70bf9.

Kennicutt, M.C., Bromwich, D., Liggett, D., Njåstad, B., Peck, L., Rintoul, S.R., Ritz, C., Siegert, M.J., Aitken, A., Brooks, C.M., Cassano, J., Chaturvedi, S., Chen, D., Dodds, K., Golledge, N.R., Le Bohec, C., Leppe, M., Murray, A., Nath, P.C., Raphael, M.N., Rogan-Finnemore, M., Schroeder, D.M., Talley, L., Travouillon, T., Vaughan, D.G., Wang, L., Weatherwax, A.T., Yang, H., Chown, S.L., 2019. Sustained Antarctic research: a 21st century imperative. One Earth 1 (1), 95–113.

Kennicutt II, M.C., Chown, S.L., Cassano, J.J., Liggett, D., Massom, R., Peck, L.S., Rintoul, S.R., Storey, J.W.V., Vaughan, D.G., Wilson, T.J., Sutherland, W.J., 2014. Polar research: six priorities for Antarctic science. Nature 512 (7512), 23–25.

Kennicutt II, M.C., Chown, S.L., Cassano, J.J., Liggett, D., Peck, L.S., Massom, R., Rintoul, S.R., Storey, J., Vaughan, D.G., Wilson, T.J., Allison, I., Ayton, J., Badhe, R., Baeseman, J., Barrett, P.J., Bell, R.E., Bertler, N., Bo, S., Brandt, A., Bromwich, D., Cary, S.C., Clark, M.S., Convey, P., Costa, E.S., Cowan, D., Deconto, R., Dunbar, R., Elfring, C., Escutia, C., Francis, J., Fricker, H.A., Fukuchi, M., Gilbert, N., Gutt, J., Havermans, C., Hik, D., Hosie, G., Jones, C., Kim, Y.D., Le Maho, Y., Lee, S.H., Leppe, M., Leitchenkov, G., Li, X., Lipenkov, V., Lochte, K., Lopez-Martinez, J., Luedecke, C., Lyons, W., Marenssi, S., Miller, H., Morozova, P., Naish, T., Nayak, S., Ravindra, R., Retamales, J., Ricci, C.A., Rogan-Finnemore, M., Ropert-Coudert, Y., Samah, A.A., Sanson, L., Scambos, T., Schloss, I.R., Shiraishi, K., Siegert, M.J., Simoes, J.C., Storey, B., Sparrow, M.D., Wall, D.H., Walsh, J.C., Wilson, G., Winther, J.G., Xavier, J.C., Yang, H., Sutherland, W.J., 2015. A roadmap for Antarctic and Southern Ocean science for the next two decades and beyond. Antarct. Sci. 27 (1), 3–18.

Le Brocq, A.M., Payne, A.J., Vieli, A., 2010. An improved Antarctic dataset for high resolution numerical ice sheet models (ALBMAP v1). Earth Syst. Sci. Data 2 (2), 247–260.

Le Brocq, A.M., Ross, N., Griggs, J.A., Bingham, R.G., Corr, H.F.J., Ferraccioli, F., Jenkins, A., Jordan, T.A., Payne, A.J., Rippin, D.M., Siegert, M.J., 2013. Evidence from ice shelves for channelized meltwater flow beneath the Antarctic Ice Sheet. Nat. Geosci. 6 (11), 945–948.

Ligtenberg, S.R.M., Helsen, M.M., van den Broeke, M.R., 2011. An improved semi-empirical model for the densification of Antarctic firn. Cryosphere 5 (4), 809–819.

Liu, H., Jezek, K.C., Li, B., Zhao, Z., 2015. Radarsat Antarctic Mapping Project Digital Elevation Model, Version 2. NASA National Snow and Ice Data Center Distributed Active Archive Center. https://doi.org/10.5067/8JKNEW6BFRVD.

Locarnini, R.A., Mishonov, A.V., Antonov, J.I., Boyer, T.P., Garcia, H.E., Baranova, O.K., Zweng, M.M., Paver, C.R., Reagan, J.R., Johnson, D.R., Hamilton, M., Seidov, D., 2013. World Ocean Atlas 2013, volume 1: temperature. In: Levitus, S., Mishonov Technical, A. (Eds.), NOAA Atlas NESDIS, vol. 73, p. 40. https://repository.library.noaa.gov/view/noaa/14847.

Matsuoka, K., Hindmarsh, R.C.A., Moholdt, G., Bentley, M.J., Pritchard, H.D., Brown, J., Conway, H., Drews, R., Durand, G., Goldberg, D., Hattermann, T., Kingslake, J., Lenaerts, J.T.M., Martín, C., Mulvaney, R., Nicholls, K.W., Pattyn, F., Ross, N., Scambos, T., Whitehouse, P.L., 2015. Antarctic ice rises and rumples: their properties and significance for ice-sheet dynamics and evolution. Earth Sci. Rev. 150, 724–745.

Mazloff, M.R., Heimbach, P., Wunsch, C., 2010. An Eddy-permitting Southern Ocean state estimate. J. Phys. Oceanogr. 40 (5), 880–899.

Mouginot, J., Scheuchl, B., Rignot, E., 2012. Mapping of ice motion in Antarctica using synthetic-aperture radar data. Rem. Sens. 4 (9), 2753–2767.

NOAA National Geophysical Data Center, 2009. ETOPO1 1 Arc-Minute Global Relief Model. NOAA National Centers for Environmental Information. https://doi.org/10.7289/V5C8276M.

Obu, J., Westermann, S., Vieira, G., Abramov, A., Balks, M.R., Bartsch, A., Hrbáček, F., Kääb, A., Ramos, M., 2020. Pan-Antarctic map of near-surface permafrost temperatures at 1 km^2 scale. Cryosphere 14 (2), 497–519.

Perkel, J.M., 2018. Map-making on a budget. Nature 558, 147–148.

Post, A.L., Meijers, A.J.S., Fraser, A.D., Meiners, K.M., Ayers, J., Bindoff, N.L., Griffiths, H.J., Van de Putte, A.P., O'Brien, P.E., Swadling, K.M., Raymond, B., 2014. Environmental setting. In: De Broyer, C., Koubbi, P., Griffiths, H.J., Raymond, B., d'Udekem d'Acoz, C., Van de Putte, A.P., Danis, B., David, B., Grant, S., Gutt, J., Held, C., Hosie, G., Huettmann, F., Post, A., Ropert-Coudert, Y. (Eds.), Biogeographic Atlas of the Southern Ocean. Scientific Committee on Antarctic Research, Cambridge UK, pp. 46–64.

Raymond, B., 2014. Pelagic regionalisation. In: De Broyer, C., Koubbi, P., Griffiths, H.J., Raymond, B., d'Udekem d'Acoz, C., Van de Putte, A.P., Danis, B., David, B., Grant, S., Gutt, J., Held, C., Hosie, G., Huettmann, F., Post, A., Ropert-Coudert, Y. (Eds.), Biogeographic Atlas of the Southern Ocean. Scientific Committee on Antarctic Research, Cambridge UK, pp. 418–421.

Rignot, E., Jacobs, S., Mouginot, J., Scheuchl, B., 2013. Ice shelf melting around Antarctica. Science 341 (6143), 266–270.

Rignot, E., Mouginot, J., Scheuchl, B., 2011. Ice flow of the Antarctic ice sheet. Science 333 (6048), 1427–1430.

Scambos, T.A., Haran, T.M., Fahnestock, M.A., Painter, T.H., Bohlander, J., 2007. MODIS-based Mosaic of Antarctica (MOA) data sets: continent-wide surface morphology and snow grain size. Remote Sens. Environ. 111 (2–3), 242–257.

Scheinert, M., Ferraccioli, F., Schwabe, J., Bell, R., Studinger, M., Damaske, D., Jokat, W., Aleshkova, N., Jordan, T., Leitchenkov, G., Blankenship, D.D., Damiani, T.M., Young, D., Cochran, J.R., Richter, T.D., 2016. New Antarctic gravity anomaly grid for enhanced geodetic and geophysical studies in Antarctica. Geophys. Res. Lett. 43 (2), 600–610.

Schiaparelli, S., Aliani, S., 2019. Oceanographic moorings as year-round laboratories for investigating growth performance and settlement dynamics in the Antarctic Scallop Adamussium Colbecki (E. A. Smith, 1902). Peerj 7. https://doi.org/10.7717/peerj.6373.

Shapiro, N.M., Ritzwoller, M.H., 2004. Inferring surface heat flux distributions guided by a global seismic model: particular application to Antarctica. Earth Planet Sci. Lett. 223 (1–2), 213–224.

Smith, B.E., Fricker, H.A., Joughin, I.R., Tulaczyk, S., 2009. An inventory of active subglacial lakes in Antarctica detected by ICESat (2003-2008). J. Glaciol. 55 (192), 573–595.

Spreen, G., Kaleschke, L., Heygster, G., 2008. Sea ice remote sensing using AMSR-E 89-GHz channels. J. Geophys. Res.: Oceans 113 (C2).

Studinger, M., Bell, R.E., Karner, G.D., Tikku, A.A., Holt, J.W., Morse, D.L., Richter, T.G., Kempf, S.D., Peters, M.E., Blankenship, D.D., Sweeney, R.E., Rystrom, V.L., 2003. Ice cover, landscape setting, and geological framework of Lake Vostok, East Antarctica. Earth Planet Sci. Lett. 205 (3–4), 195–210.

Terauds, A., 2016. An Update to the Antarctic Specially Protected Areas (ASPAs) March 2016, Ver. 1. Australian Antarctic Data Centre. https://doi.org/10.4225/15/572995579CD36.

Terauds, A., Chown, S.L., Morgan, F., Peat, H.J., Watts, D.J., Keys, H., Convey, P., Bergstrom, D.M., 2012. Conservation biogeography of the Antarctic. Divers. Distrib. 18 (7), 726–741.

Terauds, A., Lee, J.R., 2016. Antarctic biogeography revisited: updating the Antarctic Conservation Biogeographic Regions. Diversity and Distributions 22, 836–840. https://doi.org/10.1111/ddi.12453.

Tingey, R.J., 1991. 1:10 million scale Continent-wide surface schematic geological units and ages, compiled in 1985-1986. https://d28rz98at9flks.cloudfront.net/35/Bull_238.pdf.

Touzeau, A., Landais, A., Stenni, B., Uemura, R., Fukui, K., Fujita, S., Guilbaud, S., Ekaykin, A., Casado, M., Barkan, E., Luz, B., Magand, O., Teste, G., Le Meur, E., Baroni, M., Savarino, J., Bourgeois, I., Risi, C., 2016. Acquisition of isotopic composition for surface snow in East Antarctica and the links to climatic parameters. Cryosphere 10 (2), 837–852.

Treasure, A.M., Roquet, F., Ansorge, I.J., Bester, M.N., Boehme, L., Bornemann, H., Charrassin, J.B., Chevallier, D., Costa, D.P., Fedak, M.A., Guinet, C., Hammill, M.O., Harcourt, R.G., Hindell, M.A., Kovacs, K.M., Lea, M.A., Lovell, P., Lowther, A.D., Lydersen, C., McIntyre, T., McMahon, C.R., Muelbert, M.M.C., Nicholls, K., Picard, B., Reverdin, G., Trites, A.W., Williams, G.D., de Bruyn, P.J.N., 2017. Marine Mammals exploring the oceans Pole to Pole A review of the MEOP consortium. Oceanography 30 (2), 132–138.

Trusel, L.D., Frey, K.E., Das, S.B., Munneke, P.K., van den Broeke, M.R., 2013. Satellite-based estimates of Antarctic surface meltwater fluxes. Geophys. Res. Lett. 40 (23), 6148–6153.

van den Broeke, M., 2008. Depth and density of the Antarctic firn layer. Arctic Antarct. Alpine Res. 40 (2), 432–438.

van den Broeke, M., van de Berg, W.J., van Meijgaard, E., 2006. Snowfall in coastal West Antarctica much greater than previously assumed. Geophys. Res. Lett. 33, L02505.

van Wessem, J.M., Reijmer, C.H., Lenaerts, J.T.M., van de Berg, W.J., van den Broeke, M. R., van Meijgaard, E., 2014a. Updated cloud physics in a regional atmospheric climate model improves the modelled surface energy balance of Antarctica. Cryosphere 8 (1), 125–135.

van Wessem, J.M., Reijmer, C.H., Morlighem, M., Mouginot, J., Rignot, E., Medley, B., Joughin, I., Wouters, B., Depoorter, M.A., Bamber, J.L., Lenaerts, J.T.M., van de Berg, W.J., van den Broeke, M.R., van Meijgaard, E., 2014b. Improved representation of East Antarctic surface mass balance in a regional atmospheric climate model. J. Glaciol. 60 (222), 761–770.

Wright, A., Siegert, M., 2012. A fourth inventory of Antarctic subglacial lakes. Antarct. Sci. 24 (6), 659–664.

Zweng, M.M., Reagan, J.R., Antonov, J.I., Locarnini, R.A., Mishonov, A.V., Boyer, T.P., Garcia, H.E., Baranova, O.K., Johnson, D.R., Seidov, D., Biddle, M.M., 2013. World Ocean Atlas 2013, volume 2: salinity. In: Levitus, S., Mishonov Technical, A. (Eds.), NOAA Atlas NESDIS, vol. 74, p. 39.